PHILOSOPHICAL MAGAZINE LETTERS, 1999, VOL. 79, NO. 2, 79–86

Electromagnetic radiation associated with induced triaxial fracture in granite

V. FRID†, A. RABINOVITCH‡ and D. BAHAT†

† The Deichmann Rock Mechanics Laboratory of the Negev, Department of Geological and Environmental Sciences

‡ The Deichmann Rock Mechanics Laboratory of the Negev, Department of Physics, Ben Gurion University of the Negev, Beer Sheva, Israel

[*Received in final form 30 September 1998 and accepted 6 October 1998*]

ABSTRACT

A study has been made of the electromagnetic radiation (EMR) emitted during triaxial compression of granite. Changes in EMR activity with loading are shown to be strongly correlated with changes in Poisson's ratio but not with Young's modulus.

§ 1. INTRODUCTION

Although much effort has been devoted in the past to the use of electromagnetic radiation (EMR) emission for earthquake prediction (Warwick *et al.* 1982, Ogawa *et al.* 1985, Cress *et al.* 1987, Yamada *et al.* 1989, Fujinawa *et al.* 1992), such endeavours have met with very meagre success. This failure is partly due to the lack of a detailed quantitative understanding of the EMR mechanism (King 1983, Rabinovitch *et al.* 1996).

An essential requirement for this type of understanding is a careful laboratory investigation of rock failure. In a previous letter (Rabinovitch *et al.* 1998), we reported on the parametrization of individual EMR pulses and associated these parameters with crack dimensions. In this letter we discuss the correlation of EMR activity under different loading conditions with various mechanical characteristics of the material.

§ 2. EXPERIMENTAL DETAILS

2.1. *Experimental equipment*

A triaxial load frame (TerraTeck stiff press model FX-S-33090; axial pressure up to 450 MPa; confining pressure up to 70 MPa; stiffness, 5×10^9 N m^{-1}), illustrated in figure 1 was used for the measurement. It is combined with a closed-loop servocontrol (linearity, 0.05%), which is used for axial displacement monitoring during axial piston displacement. The load was measured with a sensitive load cell (LC-222M; maximum capacity, 220 kN; linearity 0.5% full scale). The confining pressure was constantly controlled by a clock-type sensor to preserve its pre-set value through volumetric changes of the sample during the loading process. The cantilever set (consisting of axial and lateral detectors; strain range, about 10%; linearity, 1% full scale) enables us to measure sample strains in three orthogonal directions parallel to the three principal stresses.

0950–0839/99 $12.00

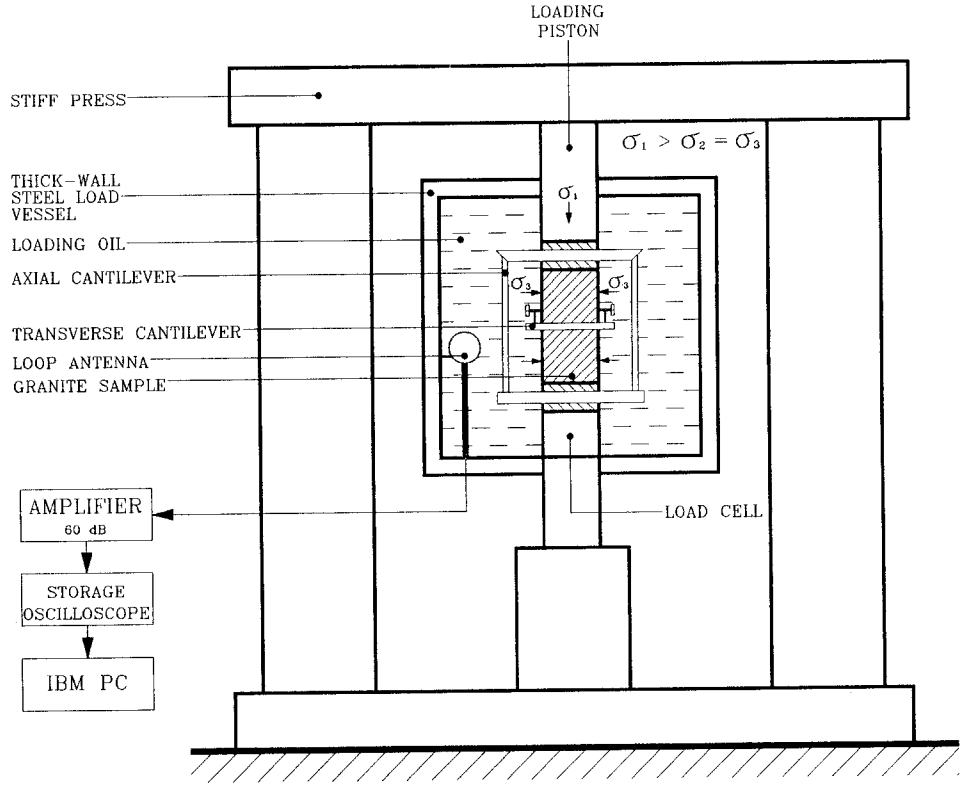

Figure 1. Schematic diagram of the experimental arrangement.

A magnetic one-loop antenna (EHFP-30 near field probe set; Electro-Metrics Penril Corporation) 3 cm in diameter was used for detection of the EMR. It is electrically small and is wound within a balanced Faraday shield which makes its response to external electric fields vanishingly small. A low-noise microsignal amplifier (Mitek Corporation Ltd; frequency range, 10 kHz–500 MHz; gain 60 ± 0.5 dB; noise level, 1.4 ± 0.1 dB across all frequency bands) and a Tektronix TDS 420 digital storage oscilloscope connected by way of a general-purpose interface bus to an IBM personal computer (PC) completed the detection equipment.

2.2. *Experimental method*

We measured the EMR inside a thick-walled steel pressure vessel in order to render the background noise level negligible. Towards this aim we also used special radio-frequency filters; the power supply for our amplifer was independent of the industrial net, and we used special double-screen cables (Alpha Wire Corporation Ltd) to connect the antenna via the amplifier to the storage oscilloscope. Our antenna–amplifier–storage oscilloscope system was completely adjusted to an input–output impedance of 50 Ω.

The antenna was situated 2 cm away from the centre of the loaded samples with its normal pointing perpendicular to the cylinder axis. We monitored the EMR activity in the frequency band from 10 kHz up to 20 MHz with an overall sensitivity of up to 1 μV.

2.3. *Sample preparation*

For our investigation we used a large Eilat granite 'block' from the Nahal Shelomo area of southern Israel, nearly 3 km from Eilat. This granite is grey and consists of K feldspars (about 40%), quartz (about 35%) albite–oligoclase (about 20%) and biotite (about 3–4%). It is medium to coarse grained (feldspars and quartz, 2–4 mm; biotite, 0.5–1 mm) and non-porphyritic (Bogosh *et al.* 1997).

All samples were cut from the granite block with unified co-orientation within the rock into standard cylinders of 100 mm length and 53 mm diameter. The density of all investigated samples was $2.604 \pm 0.005\,\mathrm{kg\,m^{-3}}$. The ends of the samples were scrupulously polished to obtain homogeneity of the stress field under compression. The end cups had a diameter identical with that of the samples. To prevent the hydrostatic loading oil from penetrating into the sample pores, all samples were enclosed in plastic jackets (Alpha Fit-221-3), and the contacts of their ends with the end cups were carefully closed. Each granite sample was tested with an axial strain rate of $1 \times 10^{-5}\,\mathrm{s^{-1}}$ and laterally by a different hydrostatical pressure. The axial pressure varied from 110 up to 284 MPa, and the confining pressure from 0 to 14 MPa.

§ 3. Deformation of rock samples and electromagnetic radiation activity

Figure 2 shows an example of a stress–strain curve of a representative granite sample (confining pressure, 10 MPa). All rock samples went through the 'normal' three deformation stages (Jaeger and Cook 1979) during compression up to the peak

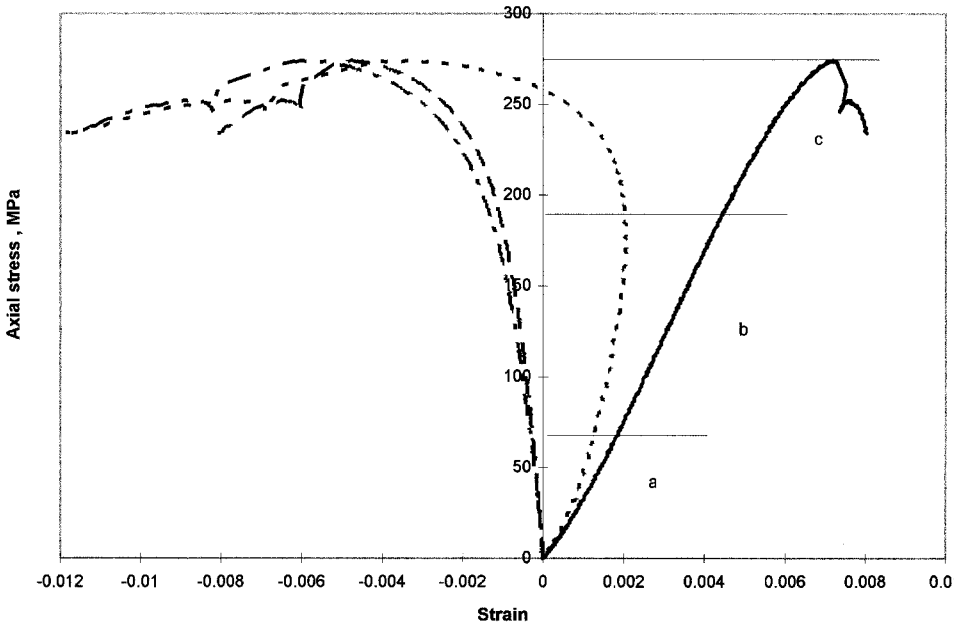

Figure 2. An example of granite triaxial deformation (confining pressure, 10 MPa) for region a, which is the pore closure region (ten EMR pulses were measured), region b, which is the elastic region (six EMR pulses were measured) and region c, which is the nonlinear region before the peak stress (eight EMR pulses were measured): (——), axial strain, (— - —), lateral strain 1; (— —), lateral strain 2; (- - -) volumetric strain.

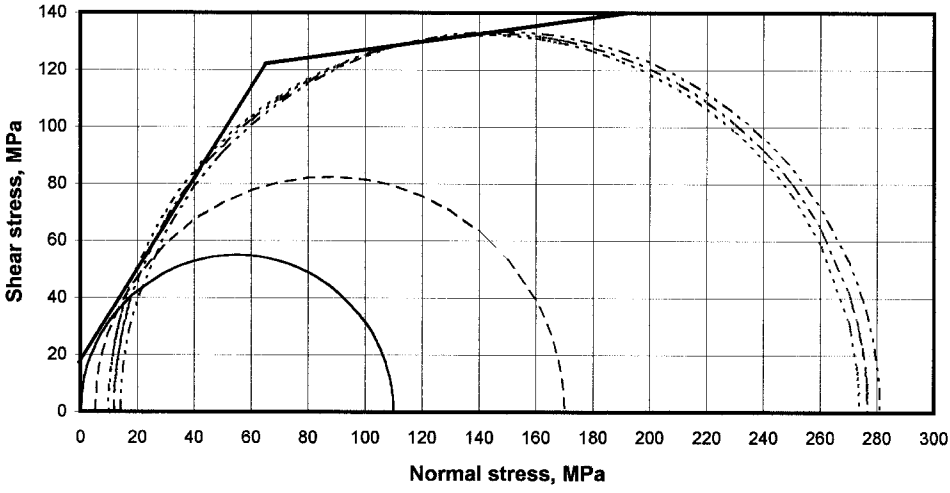

Figure 3. Two stages of the failure envelope (—) around Mohr circles which represent the different confining pressures: (——), uniaxial test; (– – –), 5 MPA confining pressure; (- - -), 10 MPa confining pressure; (– - –), 12 MPa confining pressure; (– - - –), 14 MPa confining pressure.

stress: region a, the nonlinear region of pore closure (axial strain curve here is slightly bent downwards; region b, the elastic region (the stress–strain curves are quasi-linear); region c, the nonlinear region before the peak stress.

As seen from the Mohr–Coulomb diagram (figure 3) the increase in confining pressure from 10 MPa (third circle) to 14 MPa (fifth circle) is not accompanied by an appreciable increase in shear strength (the Mohr–Coulomb envelope becomes much less steep than for a smaller confining pressure). Since the confining pressure does not cover a wide range of pressures, the ductility stage has not yet been completely reached. However, the failure plane inclination to the axial load axis was measured to be $41 \pm 1^{\circ}$. Thus, our results are reasonably close to obeying the von Mises ductile failure criteria. Poisson's ratio (figure 4(*a*)) changed from 0.36 (for the uniaxial test) via 0.27 for a 10 MPa confining pressure to 0.33 for a 14 MPa confining pressure. Young's modulus (figure 4(*b*)) increased monotonically from 27 to 48.5 GPa with increasing confining pressure.

We call the number of individual EMR pulses emitted during tracing of the entire stress–strain curve the EMR activity. Its value is seen to change with loading type (figure 4(*c*)), increasing first with increasing confining pressure and then decreasing again.

We checked the following stress–strain characteristics to investigate possible correlations with the EMR activity:

(1) the axial strain and its increment;
(2) the confining pressure;
(3) the deformation modulus (the ratio of the axial stress increment to the increase in the axial strain, i.e. secant modulus) and its absolute value;
(4) the differential stress;
(5) the differential volumetric compression work (the product of the differential stress increment and the volumetric strain changes) and its absolute value;

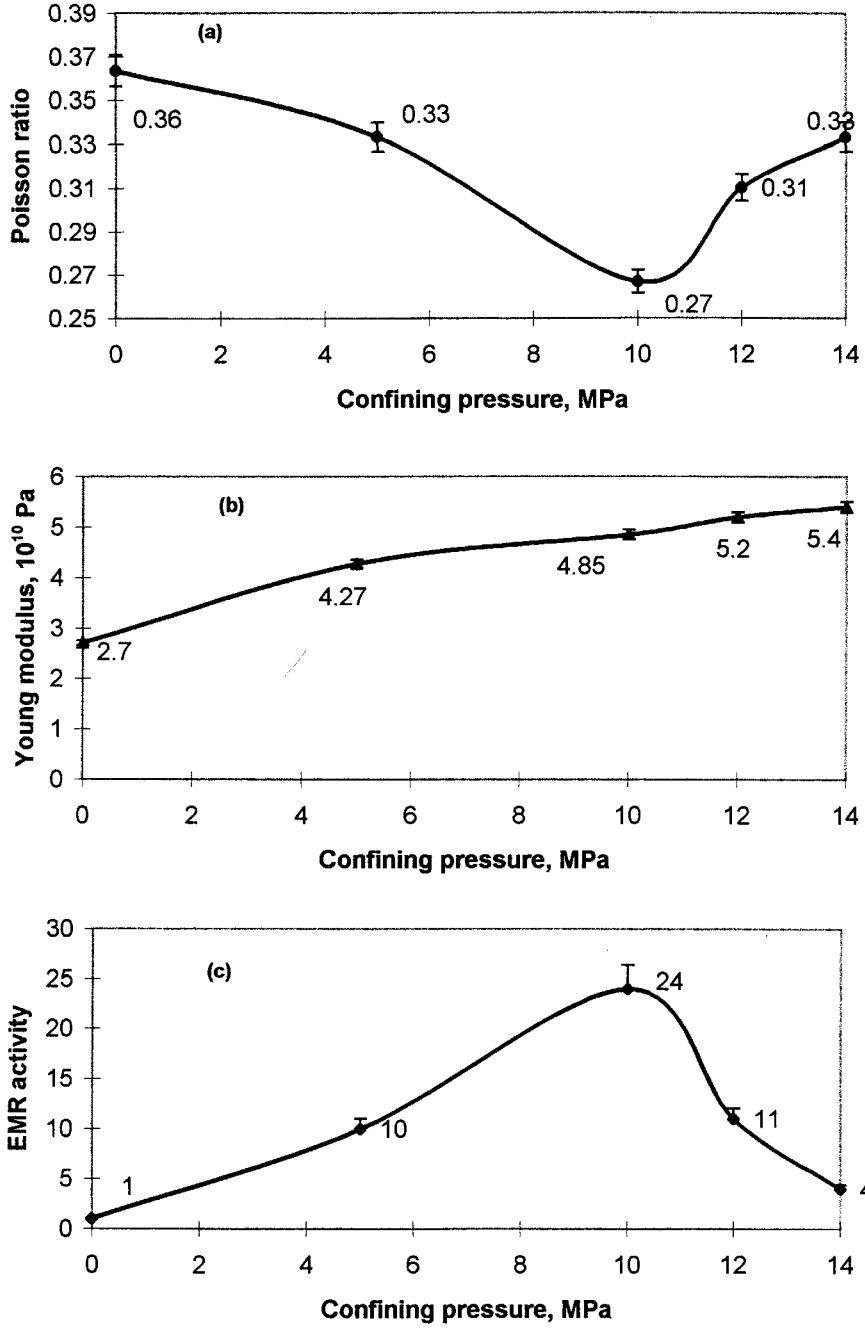

Figure 4. Relationship of the following characteristics with confining pressure: (*a*) Poisson's ratio; (*b*) Young's modulus; (*c*) the EMR activity. The error bars in these figures are determined by the accuracy limits of our rock mechanics equipment, that is ±2% for Poisson's ratio and Young's modulus (see §2.1) and by the dead time of the storage oscilloscope–IBM PC system (the period it takes for recoding, digitizing and memorizing an EMR sequence, during which the system is shut down). The error in the EMR activity is of the order of +2%.

(6) the elastic strain work (the product of the average differential stress and the elastic volumetric strain changes);
(7) the elastic volumetric strain (the part of the volumetric strain that returns to its original value after the applied stresses are removed);
(8) the lateral deformation modulus (the ratio of the axial deformation increment to the increase in lateral deformation, i.e. the secant lateral modulus) and its absolute value;
(9) the maximal stress;
(10) Poisson's ratio (the ratio of the lateral elastic deformation to the axial elastic deformation, measured in the elastic zone of deformation);
(11) the residual axial strain (axial deformation remaining after removal of external stress);
(12) the residual strain work (the strain work minus the elastic work);
(13) the residual volumetric strain (the remaining value of the sum of the three principal strains after removal of the external stress) and its absolute value;
(14) the strain work (the product of the average differential stress and the volumetric strain changes) and its absolute value;
(15) the volumetric strain (the sum of the three principal strains) and its absolute value;
(16) Young's modulus (the ratio of the axial stress increment to the increase in the elastic axial strain, measured in the elastic zone of deformation).

Note that these stress–strain characteristics can be classified as 'elastic' or 'general'. For example, Poisson's ratio and Young's modulus are defined here as elastic characteristics and measured in the elastic zone only. The lateral deformation modulus and the deformation modulus, on the other hand, are similar in definition to the Poisson's ratio and Young's modulus respectively but are 'general' characteristics; they can change during a loading process.

Our analysis shows that, of all these stress–strain characteristics, Poisson's ratio is the only one that shows good correlation with the EMR activity. Its squared regression coefficient was 0.93. An increase in Poisson's ratio (figure 4(*a*)) is accompanied by a decrease in the EMR activity (figure 4(*c*)) and vice versa. Note that, since all samples here are made of the same material (granite), Poisson's ratio varies only with loading conditions and does not vary with the material properties. Since Young's modulus increases monotonically with increasing confining pressure, it is obvious that its correlation with the EMR activity should be poor (the obtained squared regression coefficient was actually 0.18).

§ 4. Discussion

The result of a poor correlation between Young's modulus and the EMR activity is different from that found previously (Gol'd *et al.* 1975, Khatiashvilli 1984) in which an increase in Young's modulus of a material was associated with an increase in the EMR activity. In these papers, however, the correlation between Young's modulus and the EMR activity was investigated only under uniaxial compression. Our loading conditions were different. We studied changes in the EMR activity during the transition from tensional fracture (uniaxial test) via brittle shear fracture according to the Coulomb criterion, to shear fracture in the brittle–ductile region under an increase in confining pressure (for example Twiss and Moores (1992, figure 9.9)). As noted by Jaeger and Cook (1979), Young's modulus increases with

increasing confining pressure, while Poisson's ratio could both decrease and increase. We suggest that our sample deformed with increasing confining pressure as follows: an increase in the confining pressure from 0 to 10 MPa closed granite microcracks and hence Poisson's ratio was decreased to its intrinsic value of a material devoid of openings. Under a greater confining pressure (12–14 MPa), however, the deformation changed from brittle to ductile, causing an increase in Poisson's ratio. The brittle–ductile transition is confirmed by the large angle ($41 \pm 1^{\circ}$) produced between the axial load and failure plane and the insignificant increase of the shear strength (figure 3). Correspondingly, during brittle deformation, the EMR activity increased with increasing confining pressure while, in the brittle–ductile region the EMR activity decreased.

The correlation (or rather anticorrelation) of the EMR activity with Poisson's ratio seems plausible. Poisson's ratio measures the compliance of the material in the transverse direction when stressed axially. The lower Poisson's ratio is, the harder it is for the material to strain transversely, and hence the higher is the probability of new fractures (especially parallel to the axis) and of the ensuing EMR. On the other hand, the higher Poisson's ratio is, the easier it is for the material to strain transversely and, accordingly, fewer fractures and lower EMR activity should be expected. The key elastic parameter for EMR characterization during triaxial compression is therefore Poisson's ratio and not Young's modulus. Note that our results are in line with those of Gol'd *et al.* (1975) and Khatiashvilli (1984) for a uniaxial load. Our results, however, being triaxial, do show the correct global parameter to choose. They also indicate that the EMR activity correlates well with the lateral resistance to axial fracture, which is compensated by an increase in the number of new cracks.

§ 5. Summary

The correlations of changes in a wide range (23) of mechanical characteristics was checked against the EMR activity changes with loading. This allowed us to select the important characteristic germane to the EMR process, which proved to be Poisson's ratio (and not Young's modulus nor any other parameter). It seems therefore that the decrease in Poisson's ratio along the Mohr–Coulomb region correlates with a decrease in the resistance to lateral strain and an increase in fracturing and in the EMR activity. That is, the prevention of dilation directs the release of energy to increase the number of (axial) cracks. In the brittle–ductile transition region the situation is reversed; Poisson's ratio increases, the number of new cracks decreases and consequently the EMR activity diminishes.

Acknowledgements

We thank the Earth Sciences Administration of the Ministry of Energy and Infrastructure and the Koret Foundation for supporting our research. We are also grateful to Dr V. Palchik for his valuable help in conducting the experiments.

References

Bogosh, R., Bourne, J., Shirav, M., and Harnois, L., 1997, *Mineralog. Mag.*, **61**, 111.
Cress, G. O., Brady, B. T. and Rowell G. A., 1987, *Geophys. Res. Lett.*, **14**, 331.
Fujinawa, Y., Kumagai, T., and Takahashi, K., 1992, *Geophys. Res. Lett.*, **19**, 9.
Gol'd, R. M., Markov, G. P., and Mogila, P. G., 1975, *Izv. Earth Phys.*, **7**, 109.
Jaeger, J. C., and Cook, N. G. W., 1979, *Fundamentals of Rock Mechanics* (London: Chapman and Hall).

Khatiashvili, N., 1984, *Izv. Earth Phys.,* **20**, 656.
King, C. Y., 1983, *Nature,* **301**, 377.
Nitsan, V., 1977, *Geophys. Res. Lett.,* **4**, 333.
Ogawa, T., Oike, K., and Miura, T., 1985, *J. Geophys. Res.,* **90**, 6245.
Rabinovitch, A., Bahat, D., and Frid, V., 1996, *Z. Geol. Wiss.,* **24**, 361.
Rabinovitch, A., Frid, V., and Bahat, D., 1998, *Phil. Mag. Lett.,* **77**, 289.
Twiss, R. J., and Moores, E. M., 1992, *Structural Geology* (New York: Freeman).
Warwick, J. W., Stoker, C., and Meyer, T. R., 1982, *J. Geophys. Res.,* **87**, 2851.
Yamada, I., Masuda, K., and Mizutani, H., 1989, *Phys. Earth planet. Inter.,* **57**, 157.